



Contents lists available at ScienceDirect

## Bioorganic &amp; Medicinal Chemistry

journal homepage: [www.elsevier.com/locate/bmc](http://www.elsevier.com/locate/bmc)

## Synthesis and molecular docking of 1,2,3-triazole-based sulfonamides as aromatase inhibitors

Ratchanok Pingaew<sup>a,\*</sup>, Veda Prachayasittikul<sup>b</sup>, Prasit Mandi<sup>b,c</sup>, Chanin Nantasenamat<sup>b,c</sup>, Supaluk Prachayasittikul<sup>c</sup>, Somsak Ruchirawat<sup>d,e</sup>, Virapong Prachayasittikul<sup>b,\*</sup>

<sup>a</sup> Department of Chemistry, Faculty of Science, Srinakharinwirot University, Bangkok 10110, Thailand

<sup>b</sup> Department of Clinical Microbiology and Applied Technology, Faculty of Medical Technology, Mahidol University, Bangkok 10700, Thailand

<sup>c</sup> Center of Data Mining and Biomedical Informatics, Faculty of Medical Technology, Mahidol University, Bangkok 10700, Thailand

<sup>d</sup> Laboratory of Medicinal Chemistry, Chulabhorn Research Institute, and Program in Chemical Biology, Chulabhorn Graduate Institute, Bangkok 10210, Thailand

<sup>e</sup> Center of Excellence on Environmental Health and Toxicology, Commission on Higher Education (CHE), Ministry of Education, Thailand

## ARTICLE INFO

## Article history:

Received 12 February 2015

Revised 9 April 2015

Accepted 10 April 2015

Available online xxxx

## Keywords:

Triazole

Sulfonamide

Tetrahydroisoquinoline

Anti-aromatase activity

Structure–activity relationships

Molecular docking

## ABSTRACT

A series of 1,4-disubstituted-1,2,3-triazoles (**13–35**) containing sulfonamide moiety were synthesized and evaluated for their aromatase inhibitory effects. Most triazoles with open-chain sulfonamide showed significant aromatase inhibitory activity ( $IC_{50} = 1.3–9.4 \mu M$ ). Interestingly, the *meta* analog of triazole-benzene-sulfonamide (**34**) bearing 6,7-dimethoxy substituents on the isoquinoline ring displayed the most potent aromatase inhibitory activity ( $IC_{50} = 0.2 \mu M$ ) without affecting normal cell. Molecular docking of these triazoles against aromatase revealed that the compounds could snugly occupy the active site of the enzyme through hydrophobic,  $\pi$ – $\pi$  stacking, and hydrogen bonding interactions. The potent compound **34** was able to form hydrogen bonds with Met374 and Ser478 which were suggested to be the essential residues for the promising inhibition. The study provides compound **34** as a potential lead molecule of anti-aromatase agent for further development.

© 2015 Elsevier Ltd. All rights reserved.

## 1. Introduction

Breast cancer is one of the leading causes of cancer-related mortality among women worldwide from different age groups. The vast majority of breast cancers in postmenopausal women are deriving from estrogens production.<sup>1–3</sup> Estrogens are biosynthesized from androgens catalyzed by aromatase (CYP19), an enzyme belonging to the P450 family of monooxygenase heme proteins. Two main strategies to control or block breast cancer progression include binding of the estrogen receptors (ERs) with receptor antagonists (ERAs such as tamoxifen), and inhibiting the production of estrogen with aromatase inhibitors (AIs).<sup>3</sup> AIs were found to have less side effects than ERAs owing to the the lack of estrogenic activity on uterus and vasculature.<sup>3</sup>

Triazoles are common pharmacophore found in a diverse range of biologically active molecules due to their potential structural features (i.e., capability of hydrogen bonding, stable to metabolic degradation and less undesired effects).<sup>4</sup> Among the AIs, letrozole

(**1**) and anastrozole (**2**), both containing 1,2,4-triazole ring, were approved by the Food and Drug Administration (FDA) and using as the first-line therapy in the treatment of breast cancer in postmenopausal women since they have been shown to be superior to tamoxifen.<sup>3</sup> Based on the AIs, the triazole ring plays a pivotal role in chelation with heme iron.<sup>5</sup> Along the line, Touaibia group has studied on an aromatase inhibitory activity of various substituted-1,2,3-triazole letrozole-based analogs.<sup>6</sup> The results revealed that 1,2,3-triazole (**3**) analog of letrozole showed equipotent activity to the parent compound. In addition, the 1,4-disubstituted-1,2,3-triazole (**4**) was shown to be the most potent compound ( $IC_{50} = 1.36 \mu M$ ) among the tested 1,4-disubstituted-1,2,3-triazole series. Aromatase inhibitors **1–4** are shown in Figure 1. However, the interaction mode of the 1,4-disubstituted-1,2,3-triazole series with the target enzyme remains to be explored.

Recently, 1,4-disubstituted-1,2,3-triazoles bearing 1,2,3,4-tetrahydroisoquinoline (THIQ) and its open-chain derivatives **5** (Fig. 2) with cytotoxic activity against four cancer cell lines (e.g., HuCCA-1, HepG2, A549 and MOLT-3) have been reported by our group.<sup>7,8</sup> Based on the molecular docking study, an aldoketo reductase 1C3 (AKR1C3) has been identified to be a plausible target responsible for anticancer activity of the THIQ analogs.<sup>8</sup>

\* Corresponding authors. Tel.: +66 2 649 5000x18253; fax: +66 2 260 0128 (R.P.); tel.: +66 2 441 4376; fax: +66 2 441 4380 (V.P.).

E-mail addresses: [ratchanok@swu.ac.th](mailto:ratchanok@swu.ac.th) (R. Pingaew), [virapong.pra@mahidol.ac.th](mailto:virapong.pra@mahidol.ac.th) (V. Prachayasittikul).

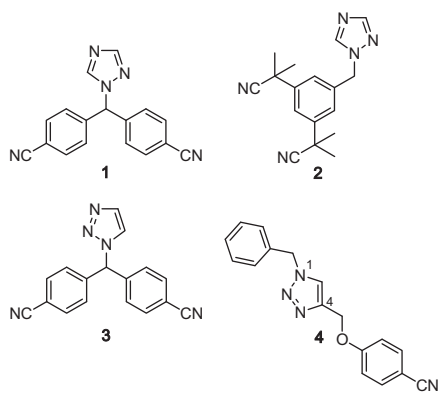


Figure 1. Aromatase inhibitors containing triazole 1–4.

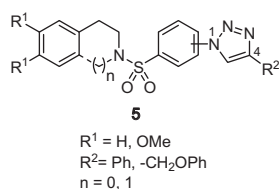


Figure 2. Cytotoxic agents containing triazole 5.

In general, two structural features of the aromatase active site associate with highly hydrophobic and H-bonding interactions.<sup>9</sup> Therefore, to design and seek for a novel class of aromatase inhibitor, many in-house 1,2,3-triazoles (series I and II) and four novel 1,2,3-triazoles of THIQ (series III) were synthesized through the Click reaction, and evaluated for their aromatase inhibitory effects. Herein, the molecules of rational designed inhibitors (Fig. 2) bearing THIQ, benzene, naphthalene and coumarin rings might be anticipated in forming hydrophobic interaction. In addition, various functional groups of the designed compounds such as

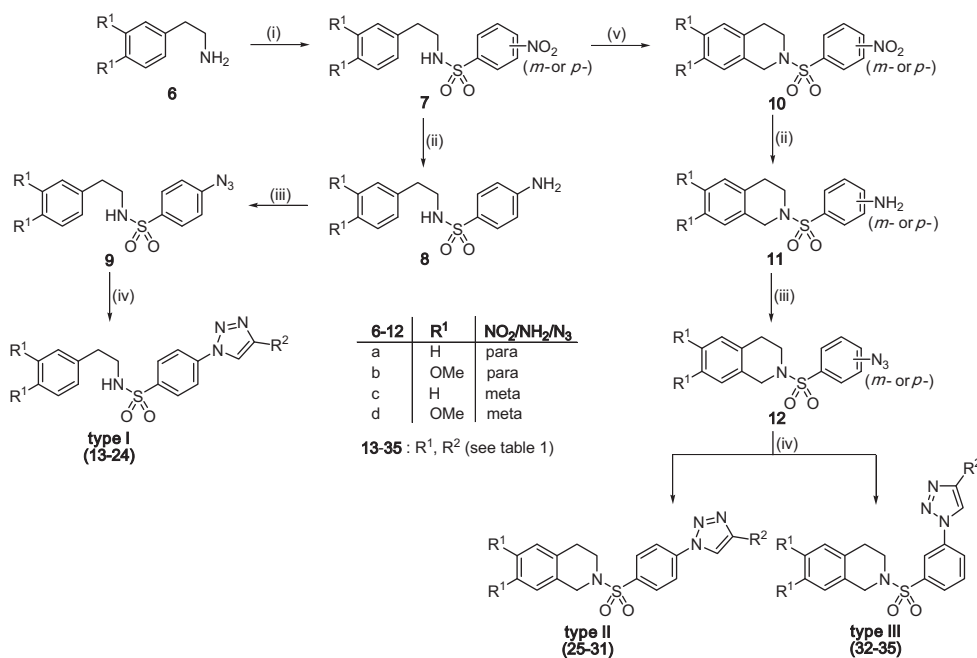
sulfonamide, triazole, ether and carbonyl moieties would participate in hydrogen bonding formation. Moreover, molecular docking of the synthesized compounds against the aromatase was also performed to give insights into their binding modes governing the investigated aromatase inhibitory activities.

## 2. Results and discussion

### 2.1. Chemistry

The synthesis of triazoles (e.g., types I and II) has been previously reported by our group.<sup>7,8</sup> The open chain THIQ analogs of triazoles **13–24** (type I) were prepared through a sequential sulfonation/reduction/diazotization/cycloaddition reactions (route a; steps i–iv) as outlined in Scheme 1. In the same manner, the synthesis of triazoles type II **25–31** and type III **32–35** was carried out via route b (steps i–v) in which an additional step (i.e., step v) was performed using the Pictet–Spengler reaction to form isoquinoline ring (**10**) prior to steps ii–iv.

Structures of the novel 1,2,3-triazoles **32–35** were confirmed based on their <sup>1</sup>H NMR, <sup>13</sup>C NMR, HRMS and IR spectra. For instance the triazole **34**, its <sup>1</sup>H NMR spectra revealed two triplets at δ 2.86 and 3.47 ppm which were assigned to the methylene protons of C4- and C3-THIQ, respectively. The methylene protons at C1-THIQ ring appeared as a singlet at δ 4.31 ppm whereas two methoxy protons at C6- and C7-positions of the THIQ part were noted as a singlet at δ 3.83 ppm. In addition, the methylene protons of –CH<sub>2</sub>O– group were found to be displayed as a singlet at δ 5.39 ppm. Aromatic protons of THIQ ring (H-5 and H-8) displayed as two singlets at δ 6.54 ppm and 6.56 ppm. Two methine protons of coumarin ring appeared as a multiplet at δ 6.92–6.98 (H-6 and H-8). The rest of three methine protons of coumarin moiety were observed as three doublets at δ 6.30 (*J* = 9.5 Hz), δ 7.39 (*J* = 9.2 Hz) and δ 7.63 (*J* = 9.5 Hz) ppm, which were assigned to methine protons of C3, C5 and C4, respectively. A triplet at δ 7.70 ppm (*J* = 8.0 Hz), two doublets at δ 7.87 (*J* = 7.8 Hz) and 7.99 ppm (*J* = 7.6 Hz) and a singlet at δ 8.17 ppm were attributed



**Scheme 1.** Synthesis of 1,2,3-triazole-based sulfonamides **13–35** through the Click reaction. Reagents and conditions: (i) 3- or 4-benzenesulfonyl chloride, Na<sub>2</sub>CO<sub>3</sub>, CH<sub>2</sub>Cl<sub>2</sub>, rt; (ii) SnCl<sub>2</sub>·2H<sub>2</sub>O, EtOH, reflux; (iii) NaNO<sub>2</sub>, HCl/CH<sub>3</sub>COOH, 0 °C, NaN<sub>3</sub>, rt; (iv) ≡–R<sup>2</sup>, CuSO<sub>4</sub>·5H<sub>2</sub>O, sodium ascorbate, *t*-BuOH/H<sub>2</sub>O, rt; (v) (CH<sub>2</sub>O)<sub>*n*</sub>, HCOOH, reflux; route a = steps i–iv; route b = steps i–v.

to four aromatic protons of benzenesulfonyl moiety. A singlet of a methine proton of the triazole ring appeared down field chemical shift at  $\delta$  8.13 ppm.

In the  $^{13}\text{C}$  NMR spectra, three methylene carbons (C1, C3 and C4) of THIQ ring were visible at  $\delta$  28.2, 43.8 and 47.2 ppm whereas a methylene carbon of  $-\text{CH}_2\text{O}-$  group was observed at  $\delta$  62.2 ppm. Two methoxy carbons (at C6 and C7) of THIQ ring were noted at 55.9 and 56.0 ppm. Two tertiary aromatic carbons of THIQ ring appeared at chemical shift 109.0 (C8) and 111.5 ppm (C5), and C5 of triazole ring was observed at  $\delta$  121.2 ppm. Five tertiary carbons (C3, C4, C5, C6 and C8) of coumarin ring were seen at chemical shift 102.2, 112.7, 113.7, 129.0 and 143.2 ppm. The rest of tertiary aromatic carbons of phenyl ring were noted at chemical shift 119.4, 124.4, 127.6 and 130.8 ppm. Four quaternary aromatic carbons (C4a, C8a, C6 and C7) of THIQ ring resonated at corresponding chemical shift 122.9, 124.8, 147.9 and 148.1 ppm, and C4 of triazole ring was observed at  $\delta$  144.5 ppm. Two quaternary aromatic carbons (C1 and C7) of phenyl ring were appeared at chemical shift 137.3 and 139.4 ppm whereas three quaternary aromatic carbons (C4a, C8a, C7) and one carbonyl carbon (C2) were observed at chemical shift 113.2, 155.8, 160.9 and 161.1 ppm.

The HRMS-TOF experiment showed molecular ion  $[\text{M}+\text{H}]^+$  peak at 575.1589 corresponding to the molecular formula of  $\text{C}_{29}\text{H}_{27}\text{N}_4\text{O}_7\text{S}$ . The IR spectra exhibited the vibration absorption bands of  $\text{C}=\text{O}$  group at  $1723\text{ cm}^{-1}$  and  $\text{S}=\text{O}$  moiety at  $1347$  and  $1163\text{ cm}^{-1}$ .

## 2.2. Biological activity

A series of 1,2,3-triazole-based sulfonamides types I–III (**13–35**), bearing disubstituents at position 1 (phenyl sulfonamide) and position 4 ( $\text{R}^2$ ), were evaluated for their aromatase inhibitory activities. All tested triazoles had inhibition effect at  $12.5\text{ }\mu\text{M}$  in the range of 14–97% (data not shown), except for compound **32** (could not be evaluated due to its insolubility in the assay). The triazoles type I (**14–20**, **22–24**) and type III (**34** and **35**) with inhibition  $>50\%$  were further explored to determine their  $\text{IC}_{50}$  values as summarized in Table 1. The derivatives with the inhibition  $\leq 50\%$  were identified as inactive compound ( $\text{IC}_{50} >12.5\text{ }\mu\text{M}$ ). Ketoconazole ( $\text{IC}_{50} = 2.6\text{ }\mu\text{M}$ ) and letrozole ( $\text{IC}_{50} = 3.3\text{ nM}$ ) were used as the reference drugs.

Results showed that sulfonamide substituents as open-chain (type I) and restricted-THIQ analogs on the phenyl ring (types II and III); and  $\text{R}^2$  substituents as phenyl, phenoxymethyl, naphthalene oxymethyl and coumarin oxymethyl on the triazole core play crucial roles in governing their anti-aromatase activities. Obviously, most of the triazoles in types I and III displayed aromatase inhibition activity ( $\text{IC}_{50} = 0.2\text{--}9.4\text{ }\mu\text{M}$ ) whereas the triazoles in type II were shown to be inactive ( $\text{IC}_{50} >12.5\text{ }\mu\text{M}$ ). Structure–activity relationship (SAR) studies of the tested compounds are discussed hereafter.

No significant inhibition effect was observed for triazole **13** ( $\text{R}^2 = \text{phenyl}$  substituent); however, triazoles bearing  $\text{R}^2$  as phenoxymethyls (**14–18**) displayed the inhibition effect with  $\text{IC}_{50}$  values in the range of  $2.9\text{--}9.4\text{ }\mu\text{M}$ . Among these compounds, 4-nitrophenoxymethyl ( $\text{R}^2$ ) analog **17** ( $\text{IC}_{50} = 2.9\text{ }\mu\text{M}$ ) exerted the highest activity having comparable  $\text{IC}_{50}$  value with that of the ketoconazole ( $\text{IC}_{50} = 2.6\text{ }\mu\text{M}$ ). When the phenyl group of compound **14** was replaced with naphthalenyl rings as found in compounds **19** and **20**, and with a 4-coumarinyl ring as found in compound **22**, the enhanced inhibitory potency was observed. In comparison between 4-coumarinyl of open-chain (**22**) and restricted THIQ (**26**) analogs ( $\text{R}^1 = \text{H}$ ), the activity was noted for compound **22** ( $\text{IC}_{50} = 1.8\text{ }\mu\text{M}$ ) but not for compound **26** ( $\text{IC}_{50} >12.5\text{ }\mu\text{M}$ ). Apparently, the triazoles **20** and **22** exerted inhibition activity higher than that of the ketoconazole. On the other hand, the

triazole was substituted with 7-coumarinoxymethyl substituent ( $\text{R}^2$ ) led to the compound **21** with loss of the activity as compared to the 4-coumarinyl group of compound **22** ( $\text{IC}_{50} = 1.8\text{ }\mu\text{M}$ ). Inhibition potency was distinctively appeared as noted in compound **23** ( $\text{IC}_{50} = 4.6\text{ }\mu\text{M}$ ) when dimethoxy groups ( $\text{R}^1$ ) were introduced to 3,4-positions on phenethyl moiety of analog **13** ( $\text{R}^1 = \text{H}$ ,  $\text{IC}_{50} >12.5\text{ }\mu\text{M}$ ). However, no aromatase inhibition was observed for triazole type II (**25–31**) containing  $\text{R}^1 = \text{H}$  and  $\text{OMe}$  on the THIQ. Both triazole types I and II constituting sulfonyl group at *para* position on phenyl ring, anti-aromatase activity was observed for type I compounds, except for compounds **13** and **21** ( $\text{IC}_{50} >12.5\text{ }\mu\text{M}$ ). Surprisingly, when the sulfonyl group on the phenyl ring was moved to *meta* position, the activity of compounds was remarkably manifested. Promisingly, 7-coumarinyl analog **34** ( $\text{R}^1 = \text{OMe}$ ) was shown to be the most potent compound with  $\text{IC}_{50}$  value of  $0.2\text{ }\mu\text{M}$ . Potent activity was also found in dimethoxy THIQ of 4-coumarinyl analog **35** ( $\text{R}^1 = \text{OMe}$ ,  $\text{IC}_{50} = 1.8\text{ }\mu\text{M}$ ). However, without 6,7-dimethoxy groups on the THIQ ring, 4-coumarinyl analog **33** ( $\text{R}^1 = \text{H}$ ) was shown to be an inactive aromatase inhibitor.

The SAR results imply that lipophilic effect of dimethoxy groups ( $\text{R}^1$ ) enhances the activity of triazoles type I and type III. Our results are in-line with earlier studies, in which the lipophilicity is responsible for high aromatase inhibition of xanthone<sup>10</sup> and coumarin<sup>11</sup> derivatives. Even with or without dimethoxy groups, the triazoles type II with restricted THIQ were shown to be inactive compounds. This could be possibly due to their structural features, that is, flexible or rigid conformation, isomeric effect and binding interaction with the target site of action. Therefore, the aid of molecular docking may provide insight into their mechanism of action.

To determine the safety index, these compounds were also tested against the noncancerous (Vero) cell line derived from African green monkey kidney (Table 1). It was found that the potent analogs (**14–20**, **22–24**, **34** and **35**) were non-cytotoxic toward normal cell, except for compound **35**. However, the triazole **35** had high safety index with a selective index value of 48.

## 2.3. Molecular docking

Molecular docking of triazoles **13–35** to the aromatase enzyme was performed to investigate their binding modes. The most potent compound **34** (Fig. 3) was able to form hydrogen bonds with Met374 and Ser478 using the sulfonyl oxygen (bond distance =  $2.3\text{ \AA}$ ) and the oxycoumarinyl group (bond distance =  $2.0\text{ \AA}$ ), respectively. The 2D ligand–protein interaction map of the co-crystallized ligand ASD (Fig. S1) displayed hydrophobic interaction involving steroidal backbone with amino acids residues (i.e., Ile133, Phe134, Trp224 and Leu477), and hydrogen bonding of the CO group at position 17 with the amino group of Met374.

Interestingly, isomeric coumarinyl and naphthalenyl triazoles play crucial roles in exerting more potent aromatase inhibitory activity than other tested compounds. This could be attributed to their binding interactions with the aromatase enzyme. Docking results (Figs. S2 and S3) of 4-coumarinyl triazoles (**22** and **35**) with the same potency ( $\text{IC}_{50} = 1.8\text{ }\mu\text{M}$ ) showed that compound **22** occupied the binding cavity in a more straight extended form when compared with that of compound **35**. The binding of compound **22** (Fig. S2) facilitated hydrophobic interaction of phenethyl phenylsulfonamide moiety with Ile133, Val370, Ser478, Thr310 and Trp224 along with the interaction of 4-coumarinyl ring with Phe221;  $\pi$ – $\pi$  stacking interaction of triazole and 4-coumarinyl rings with Phe221; and hydrogen bonding of coumarin-2-one with the amino group of Arg192. Docking of triazole **35** (Fig. S3) involves hydrophobic interactions of dimethoxy THIQ with Ile133, of sulfonyl phenyl with Asp309 and Thr310 as well as of the

**Table 1**  
Aromatase inhibitory activity and cytotoxic activity (IC<sub>50</sub>, μM) of triazoles (13–35)

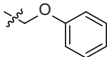
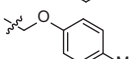
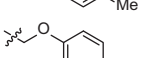
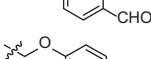
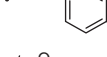
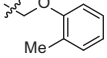
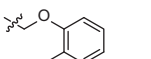
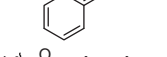
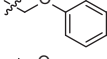
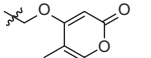
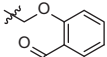
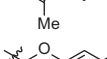
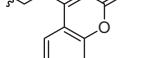
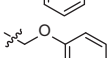
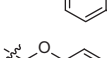
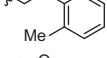
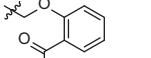
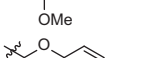
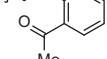
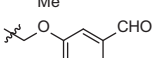
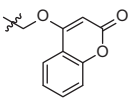
Series	Compound	R <sup>1</sup>	R <sup>2</sup>	Inhibitory activity (aromatase)	Cytotoxic activity (Vero cell line)	Selective index <sup>a</sup>	
I	13	H		>12.5	Non-cytotoxic	–	
	14	H		9.4 ± 1.6	Non-cytotoxic	>12.24	
	15	H		8.0 ± 0.2	Non-cytotoxic	>13.93	
	16	H		7.9 ± 0.7	Non-cytotoxic	>13.68	
	17	H		2.9 ± 0.1	Non-cytotoxic	>35.96	
	18	H		3.4 ± 0.1	Non-cytotoxic	>32.79	
	19	H		3.4 ± 1.5	Non-cytotoxic	>30.35	
	20	H		1.3 ± 0.4	Non-cytotoxic	>79.37	
	21	H		>12.5	Non-cytotoxic	–	
	22	H		1.8 ± 0.5	Non-cytotoxic	>55.27	
	23	OMe	H		4.6 ± 2.0	Non-cytotoxic	>23.40
	24	OMe	H		2.7 ± 0.1	Non-cytotoxic	>34.32
	II	25	H		>12.5	Non-cytotoxic <sup>b</sup>	–
26		H		>12.5	28.58 <sup>b</sup>	–	
27		OMe	H		>12.5	Non-cytotoxic <sup>b</sup>	–
28		OMe	H		>12.5	Non-cytotoxic <sup>b</sup>	–
29		OMe	H		>12.5	2.82 <sup>b</sup>	–
30		OMe	H		>12.5	37.23 <sup>b</sup>	–
31		OMe	H		>12.5	Non-cytotoxic <sup>b</sup>	–
III		32	H		– <sup>c</sup>	91.54	–
	33	H		>12.5	Non-cytotoxic	–	
	34	OMe		0.2 ± 0.1	Non-cytotoxic	>435.09	

Table 1 (continued)

Series	Compound	R <sup>1</sup>	R <sup>2</sup>	Inhibitory activity (aromatase)	Cytotoxic activity (Vero cell line)	Selective index <sup>a</sup>
	<b>35</b>	OMe		1.8 ± 0.2	86.32	47.96
	Ketoconazole <sup>d</sup>			2.6 ± 0.7	—	—
	Letrozole <sup>d</sup>			0.0033 ± 0.0004	—	—
	Ellipticine <sup>d</sup>			—	1.94	—

Vero cell line = African green monkey kidney cell line.

Non-cytotoxic = IC<sub>50</sub> > 50 µg/mL.

<sup>a</sup> Selective index = IC<sub>50</sub> for Vero cells/IC<sub>50</sub> for aromatase.

<sup>b</sup> Data from reference number 8.

<sup>c</sup> Insoluble in testing medium

<sup>d</sup> Ketoconazole, letrozole and ellipticine were used as reference drugs.

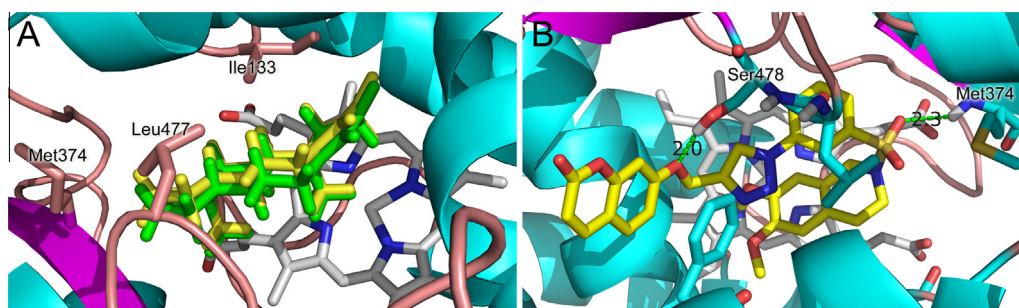


**Figure 3.** Molecular docking of 1,2,3-triazole sulfonamides to aromatase enzyme. Redocking of co-crystallized androstenedione (ASD) yielded RMSD of 0.711 Å (A). Docking pose of the most potent compound **34** (B) is shown where green dashed lines indicate distances of hydrogen bonds.

4-coumarinyl ring with Phe221 and His480. This molecular arrangement induced  $\pi$ - $\pi$  stacking of phenylsulfonyl, triazole and 4-coumarinyl rings with Phe221; and hydrogen bonding of triazole (N3 position) with Ser478, and oxycoumarinyl moiety with Arg192. Such interactions involve molecules in the bent form (**35**), which arises from *m*-substitution of the sulfonyl group and triazole ring on the phenyl ring of sulfonamide. The results suggested that the Ser478 and Arg192 residues were essential for the inhibition of aromatase. It should be noted that both Ser478 and Arg192 played crucial roles in anti-aromatase activity of the natural substrate ASD.<sup>9</sup> Accordingly, such amino acids participated in a water-mediated network of hydrogen bonding, thereby allowing the interaction between the aromatase and the C3-keto oxygen of androstenedione to undergo enolization.<sup>9</sup> Furthermore, Ser478 was capable of promoting the aromatase inhibition confirmed by the mutagenesis study.<sup>12</sup> In addition, such amino acid was the residue responsible for the inhibition and selectivity.<sup>13,14</sup>

The triazole **26** (Fig. S4), a restricted THIQ analog of **22**, similarly showed hydrophobic and  $\pi$ - $\pi$  stacking interactions with the aromatase. The triazole **21** (Fig. S5), an isomeric analog of **22**, showed that both terminal ends (phenethyl and 7-coumarinyl) could interact with the hydrophobic pockets. However, no hydrogen bonding with Arg192 was noted for compounds **26** and **21**. This could likely result in the absence of inhibitory activity for the compounds **26** and **21** (IC<sub>50</sub> > 12.5 µM) as compared to that of compound **22** (IC<sub>50</sub> 1.8 µM).

Comparison of THIQs with 4-coumarinyl moiety **33** (R<sup>1</sup> = H, Fig. S6) and **35** (R<sup>1</sup> = OMe, Fig. S3) revealed that both compounds displayed similar hydrophobic and hydrogen bonding interactions with the binding pockets of the aromatase. It was observed that lipophilic dimethoxy groups were essential for the interaction of

compound **35** with Ile133 in exerting its activity (IC<sub>50</sub> = 1.8 µM) while compound **33** without dimethoxy groups was shown to be an inactive compound (IC<sub>50</sub> > 12.5 µM).

Considering the most potent dimethoxy THIQ bearing 7-coumarinyl analog **34** (Fig. 4), additional hydrophobic interactions with Val370, Ser478, Leu477 and Trp224 were observed as compared to compound **35** (Fig. S3). Furthermore, the compound **34** was arranged in such a way to appropriately form hydrogen bonding of the sulfonyl group with the amino group of Met374 as well as hydrogen bonding of oxycoumarinyl moiety with Ser478. These hydrophobic and hydrogen bonding interactions were suggested to play pertinent roles contributing to the most potent activity of

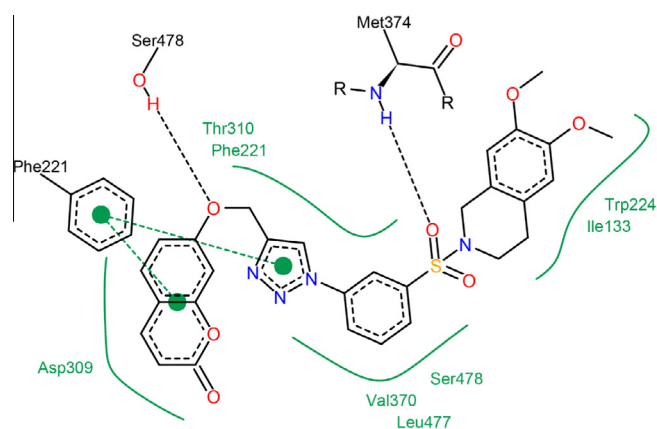


**Figure 4.** 2D-ligand-protein interaction scheme of compound **34**.

compound **34** ( $IC_{50} = 0.2 \mu\text{M}$ ). Importantly, Leu477 and Trp224 were the same hydrophobic residues interacting with steroidal skeleton of ASD (Fig. S1). The H-bonding formations with Ser478 and Met374 (bond distance = 3.11 and 2.31 Å) were also noted in the antiestrogenic letrozole in which it used two benzonitrile groups to form such interactions.<sup>15</sup> However, the compound **34** showed lower potency than letrozole. This may be due to the lack of chelation with heme iron. Notably, the Met374 played a crucial role in anti-aromatase activity of the natural substrate ASD through H-bonding interaction with the C17-keto oxygen.<sup>9</sup> In addition, Met374 and/or Ser478 were suggested to be the crucial residues found in many classes of aromatase inhibitors such as coumarin,<sup>11</sup> acridone,<sup>13</sup> xanthone<sup>14</sup> and flavonoids.<sup>16,17</sup>

Unfortunately, 7-coumarinyl analog **32** ( $R^1 = \text{H}$ ) was not tested for the activity due to its insolubility in the testing system. Therefore, the activity of 7-coumarinyl **32** cannot be compared with 7-coumarinyl **34** ( $R^1 = \text{OMe}$ , Fig. 4). However, the 2D ligand–protein interaction of **32** (Fig. S7) showed hydrophobic and  $\pi$ – $\pi$  stacking interactions but without hydrogen bond forming.

In addition, the analysis of triazole type I analog of naphthalenyl ( $R^2$ ), particularly the highly potent 2-naphthalenyl compound **20** (Fig. S8), was found to be in the extended form when occupying the binding site via hydrophobic interaction of phenethyl with Ile133, Val370 and Thr310, phenyl sulfonyl with Leu477 and Ser478 as well as 2-naphthalenyl with Phe221, Asp309 and His480; through  $\pi$ – $\pi$  stacking of triazole and naphthalenyl rings with Phe221; and hydrogen bonding of oxy-naphthalenyl moiety with Ser478. On the other hand, the less extended form of 1-naphthalenyl compound **19** (Fig. S9) showed hydrophobic interaction of phenethyl phenyltriazole with Ile133, Thr310, Phe221, Ser478 and Asp309 as well as 1-naphthalenyl ring with Gln218;  $\pi$ – $\pi$  stacking of triazole and 1-naphthalenyl rings with Phe221; but no hydrogen bonding was observed. The results implied that the presence of H-bonding interaction with Ser478 contributed to the better activity of compound **20** ( $IC_{50} = 1.3 \mu\text{M}$ ) over compound **19** ( $IC_{50} = 3.4 \mu\text{M}$ ).

Taken together, the molecular requirements for the most potent triazole inhibitor (**34**) included the restricted THIQ with 6,7-dimethoxy groups ( $R^1$ ), 7-coumaryloxymethyl ( $R^2$ ) at position 4 of the triazole ring, and *m*-substitution of triazole and sulfonyl moieties on the phenyl ring. Such structural features were essential for engaging in hydrophobic,  $\pi$ – $\pi$  stacking and H-bonding interactions with the aromatase enzyme, particularly, hydrogen bond forming with Met374 and Ser478. Obviously, triazole **34** was the only compound that engaged in the hydrogen bonding interactions. In comparison with letrozole and ASD, the sulfonyl and coumarinyl ether moieties of compound **34** could act as hydrogen bond acceptors to mimic the benzonitrile groups of the letrozole whereas mimicking the steroidal backbone and the C17-keto oxygen of ASD was responsible by the hydrophobic moieties (6,7-dimethoxy THIQ and phenyl rings) and the sulfonyl oxygen of compound **34**, respectively.

### 3. Conclusions

A series of 1,2,3-triazole-based sulfonamides (**13–35**) have been synthesized using the Click reaction as a key step. Their aromatase inhibitory activities and molecular docking were explored. It was observed that most open-chain sulfonamide triazoles (Type I) exerted aromatase inhibitory activity ( $IC_{50} = 1.3–9.4 \mu\text{M}$ ). All triazoles (Type II) with restricted THIQ analogs were shown to be inactive compounds. The triazoles **34** and **35** displayed potent activity where they contained 6,7-dimethoxy substituents ( $R^1$ ) on the THIQ core, and coumarinyloxymethyl ( $R^2$ ) on the triazole ring; and *m*-substitution of sulfonyl group and triazole ring on the phenyl moiety of sulfonamide. Particularly, the triazole **34** was shown to be

the most potent inhibitor ( $IC_{50} = 0.2 \mu\text{M}$ ) without affecting the normal cell line. Moreover, the molecular docking study revealed that the investigated triazoles could snugly occupy the active site of aromatase through the interactions of hydrophobic,  $\pi$ – $\pi$  stacking and H-bonding. The most potent compound (**34**) was the only one that displayed H-bonding interactions with both Met374 and Ser478 which were suggested to be the essential amino acid residues for the inhibitory activity.

## 4. Experimental

### 4.1. Chemistry

Column chromatography was carried out using silica gel 60 (70–230 mesh ASTM). Analytical thin-layer chromatography (TLC) was performed with silica gel 60 F<sub>254</sub> aluminum sheets. <sup>1</sup>H and <sup>13</sup>C NMR spectra were recorded on a Bruker AVANCE 300 NMR spectrometer (operating at 300 MHz for <sup>1</sup>H and 75 MHz for <sup>13</sup>C). The following standard abbreviations were used for signal multiplicities: singlet (s), doublet (d), triplet (t), quartet (q) and multiplet (m). FTIR spectra were obtained using a universal attenuated total reflectance attached on a Perkin–Elmer Spectrum One spectrometer. Mass spectra were recorded on a Bruker Daltonics (microTOF). Melting points were determined using a Griffin melting point apparatus and were uncorrected.

Data associated with the compounds **13–31** were reported in our previous work.<sup>7,8</sup>

### 4.2. General procedure for the synthesis of nitrobenzenesulfonamides (7c–d)

A solution of phenylethylamine **6** (10 mmol) in dichloromethane (50 mL) was added dropwise to a stirred mixture of 3-nitrobenzenesulfonyl chloride (10 mmol) and sodium carbonate (14 mmol) in dichloromethane (20 mL). The reaction mixture was stirred at room temperature overnight, and added distilled water (20 mL). The organic phase was separated and the aqueous phase was extracted with dichloromethane (2 × 30 mL). The organic extracts were combined and washed with water (30 mL). The organic layer was dried over anhydrous sodium sulfate (anhyd Na<sub>2</sub>SO<sub>4</sub>), filtered and evaporated to dryness under reduced pressure. The crude product was further purified by recrystallization.

<sup>1</sup>H NMR of 3-nitro-*N*-phenethylbenzenesulfonamide (**7c**) was consistent with that reported in the literature.<sup>18</sup>

#### 4.2.1. *N*-(3,4-Dimethoxyphenethyl)-3-nitrobenzenesulfonamide (7d)

Pale yellow solid. 87%. Mp 103–104 °C. IR (UATR)  $\text{cm}^{-1}$ : 3233, 1607, 1592, 1534, 1332, 1162  $\text{cm}^{-1}$ . <sup>1</sup>H NMR (300 MHz, CDCl<sub>3</sub>)  $\delta$  2.77 (t, *J* = 6.6 Hz, 2H, ArCH<sub>2</sub>), 3.31 (q, *J* = 6.6 Hz, 2H, CH<sub>2</sub>NH), 3.82, 3.86 (s, 6H, 2 × OCH<sub>3</sub>), 4.65 (br t, 1H, NH), 6.58 (s, 1H, ArH), 6.64 (d, *J* = 8.1 Hz, 1H, ArH), 6.76 (d, *J* = 8.1 Hz, 1H, ArH), 7.70 (t, *J* = 8.0 Hz, 1H, ArH), 8.10 (d, *J* = 8.0 Hz, 1H, ArH), 8.43 (d, *J* = 8.1 Hz, 1H, ArH), 8.62 (s, 1H, ArH). <sup>13</sup>C NMR (75 MHz, CDCl<sub>3</sub>):  $\delta$  35.5, 44.5, 55.8, 55.9, 111.4, 111.7, 120.8, 122.2, 127.0, 130.0, 130.3, 132.4, 142.3, 148.1, 148.3, 149.2. HRMS-TOF: *m/z* [M+H]<sup>+</sup> 367.0957 (Calcd for C<sub>16</sub>H<sub>19</sub>N<sub>2</sub>O<sub>6</sub>S: 367.0958).

### 4.3. General procedure for the synthesis of 1,2,3,4-tetrahydroisoquinolines (10c–d)

A mixture of sulfonamide **7** (6.7 mmol) and paraformaldehyde (7.2 mmol) in formic acid (30 mL) was refluxed for 2 h, and then allowed to cool to room temperature. The reaction mixture was added to 30 mL of water, and the product was extracted with

CH<sub>2</sub>Cl<sub>2</sub> (2 × 30 mL). Combined extracts were washed with saturated aqueous NaHCO<sub>3</sub>, dried (anhyd Na<sub>2</sub>SO<sub>4</sub>) and evaporated to dryness under reduced pressure. The crude product was recrystallized from methanol.

<sup>1</sup>H NMR of 2-((3-nitrophenyl)sulfonyl)-1,2,3,4-tetrahydroisoquinoline (**10c**) was consistent with that reported in the literature.<sup>19</sup>

#### 4.3.1. 6,7-Dimethoxy-2-((3-nitrophenyl)sulfonyl)-1,2,3,4-tetrahydroisoquinoline (**10d**)

Pale yellow solid. 80%. Mp 133–134 °C. IR (UATR) cm<sup>-1</sup>: 1611, 1532, 1519, 1351, 1175, 1117. <sup>1</sup>H NMR (300 MHz, CDCl<sub>3</sub>) δ 2.86 (t, *J* = 5.8 Hz, 2H, C4-H), 3.47 (t, *J* = 5.8 Hz, 2H, C3-H), 3.84 (s, 6H, 2 × OCH<sub>3</sub>), 4.30 (s, 2H, C1-H), 6.54, 6.55 (2s, 2H, C-5, C-8), 7.76 (t, *J* = 8.1 Hz, 1H, ArH), 8.16 (d, *J* = 7.7 Hz, 1H, ArH), 8.44 (d, *J* = 8.0 Hz, 1H, ArH), 8.68 (s, 1H, ArH). <sup>13</sup>C NMR (75 MHz, CDCl<sub>3</sub>) δ 28.1, 43.8, 47.2, 55.9, 56.0, 108.9, 111.4, 122.7, 124.6, 127.2, 130.5, 132.9, 139.4, 147.9, 148.1, 148.3. HRMS-TOF: *m/z* [M+Na]<sup>+</sup> 401.0768 (Calcd for C<sub>17</sub>H<sub>18</sub>N<sub>2</sub>NaO<sub>6</sub>S: 401.0778).

#### 4.4. General procedure for the synthesis of 1,2,3,4-tetrahydroisoquinolines (**11c–d**)

A mixture of nitroisoquinoline **10** (4 mmol) and SnCl<sub>2</sub>·2H<sub>2</sub>O (40 mmol) in absolute ethanol (20 mL) was stirred under reflux for 4 h then concentrated under reduced pressure. Water (20 mL) was added and extracted with EtOAc (3 × 20 mL). The organic extracts were combined and washed with water (20 mL) and brine (20 mL). The organic layer was dried over anhyd Na<sub>2</sub>SO<sub>4</sub>, filtered and concentrated. The crude product was recrystallized from methanol.

<sup>1</sup>H NMR of 2-((3-aminophenyl)sulfonyl)-1,2,3,4-tetrahydroisoquinoline (**11c**) was consistent with that reported in the literature.<sup>19</sup>

#### 4.4.1. 2-((3-Aminophenyl)sulfonyl)-6,7-dimethoxy-1,2,3,4-tetrahydroisoquinoline (**11d**)

Pale yellow solid. 80%. Mp 170–171 °C. IR (UATR) cm<sup>-1</sup>: 3468, 3374, 1626, 1599, 1519, 1317, 1158, 1117. <sup>1</sup>H NMR (300 MHz, DMSO-*d*<sub>6</sub>) δ 2.76 (t, *J* = 5.8 Hz, 2H, C4-H), 3.18 (t, *J* = 5.8 Hz, 2H, C3-H), 3.64 (s, 6H, 2 × OCH<sub>3</sub>), 4.00 (s, 2H, C1-H), 5.62 (s, 2H, NH<sub>2</sub>), 6.67, 6.72 (2s, 2H, C-5, C-8), 6.80 (dd, *J* = 8.0, 1.3 Hz, 2H, ArH), 6.85 (d, *J* = 8.0 Hz, 1H, ArH), 6.97 (s, 1H, ArH), 7.22 (t, *J* = 7.8 Hz, 1H, ArH). <sup>13</sup>C NMR (75 MHz, DMSO-*d*<sub>6</sub>) δ 28.2, 44.2, 47.4, 56.0, 110.0, 110.3, 112.1, 112.3, 114.5, 118.4, 123.7, 125.3, 130.2, 147.8, 148.0, 150.0. HRMS-TOF: *m/z* [M+Na]<sup>+</sup> 371.1039 (Calcd for C<sub>17</sub>H<sub>20</sub>N<sub>2</sub>NaO<sub>4</sub>S: 371.1036).

#### 4.5. General procedure for the synthesis of 2-((3-azidophenyl)sulfonyl)-1,2,3,4-tetrahydroisoquinolines (**12c–d**)

To a cold solution of amine **11** (3 mmol) in HCl/CH<sub>3</sub>COOH (3:3 mL) at 0 °C, a solution of sodium nitrite (9 mmol) in water (5 mL) was added. The stirred reaction mixture was maintained for 15 min and then added dropwise a solution of sodium azide (9 mmol) in water (5 mL). The reaction mixture was allowed to stir at room temperature for 0.5 h, then the precipitate was filtered and washed with cold water. The crude product was recrystallized from methanol.

#### 4.5.1. 2-((3-Azidophenyl)sulfonyl)-1,2,3,4-tetrahydroisoquinoline (**12c**)

Pale yellow solid. 94%. Mp 120–121 °C. IR (UATR) cm<sup>-1</sup>: 2154, 2109, 1595, 1337, 1169. <sup>1</sup>H NMR (300 MHz, CDCl<sub>3</sub>) δ 2.93 (t,

*J* = 6.0 Hz, 2H, C4-H), 3.42 (t, *J* = 6.0 Hz, 2H, C3-H), 4.31 (s, 2H, C1-H), 7.02–7.18 (m, 4H, ArH), 7.22 (d, *J* = 7.9 Hz, 1H, ArH), 7.47 (s, 1H, ArH), 7.51 (t, *J* = 7.9 Hz, 1H, ArH), 7.60 (d, *J* = 7.8 Hz, 1H, ArH). <sup>13</sup>C NMR (75 MHz, CDCl<sub>3</sub>) δ 28.7, 43.7, 47.5, 118.0, 123.1, 123.7, 126.3, 126.5, 126.9, 128.8, 130.5, 131.4, 133.0, 138.8, 141.6. HRMS-TOF: *m/z* [M+Na]<sup>+</sup> 337.0737 (Calcd for C<sub>15</sub>H<sub>14</sub>N<sub>4</sub>NaO<sub>2</sub>S: 337.0730).

#### 4.5.2. 2-((3-Azidophenyl)sulfonyl)-6,7-dimethoxy-1,2,3,4-tetrahydroisoquinoline (**12d**)

Pale yellow solid. 85%. Mp 86–87 °C. IR (UATR) cm<sup>-1</sup>: 2155, 2106, 1592, 1518, 1465, 1346, 1167, 1116. <sup>1</sup>H NMR (300 MHz, CDCl<sub>3</sub>) δ 2.81 (t, *J* = 5.8 Hz, 2H, C4-H), 3.37 (t, *J* = 5.8 Hz, 2H, C3-H), 3.80 (s, 6H, 2 × OCH<sub>3</sub>), 4.20 (s, 2H, C1-H), 6.50, 6.53 (s, 2H, ArH), 7.21 (d, *J* = 7.7 Hz, 1H, ArH), 7.44 (s, 1H, ArH), 7.48 (t, *J* = 7.9 Hz, 1H, ArH), 7.56 (d, *J* = 7.7 Hz, 1H, ArH). <sup>13</sup>C NMR (75 MHz, CDCl<sub>3</sub>) δ 28.3, 43.8, 47.2, 55.9, 56.0, 109.0, 111.5, 118.0, 123.1, 123.7, 124.9, 130.5, 141.5, 147.9, 148.1. HRMS-TOF: *m/z* [M+Na]<sup>+</sup> 397.0925 (Calcd for C<sub>17</sub>H<sub>18</sub>N<sub>4</sub>NaO<sub>4</sub>S: 397.0941).

#### 4.6. General procedure for the synthesis of triazoles (**32–35**)

To a stirred solution of azido **12** (0.2 mmol) and the corresponding alkyne (0.2 mmol) in *t*-BuOH/H<sub>2</sub>O (3:3 mL), CuSO<sub>4</sub>·5H<sub>2</sub>O (0.2 mmol) and ascorbic acid (0.5 mmol) were added. The reaction mixture was stirred at room temperature for 2–12 h (monitored by TLC), then concentrated under reduced pressure. The residue was added water (10 mL) and extracted with dichloromethane (3 × 20 mL). The combined organic phases were washed with water (20 mL), dried over anhyd Na<sub>2</sub>SO<sub>4</sub> and evaporated to dryness. The crude product was purified using silica gel column chromatography and eluted with methanol/dichloromethane (1:50).

#### 4.6.1. 7-((1-(3-((3,4-Dihydroisoquinolin-2(1H)-yl)sulfonyl)phenyl)-1H-1,2,3-triazol-4-yl)methoxy)-2H-chromen-2-one (**32**)

White solid. 88%. Mp 180–181 °C. IR (UATR) cm<sup>-1</sup>: 1725, 1616, 1486, 1342, 1229, 1163, 1127. <sup>1</sup>H NMR (300 MHz, CDCl<sub>3</sub>) δ 2.95 (t, *J* = 5.9 Hz, 2H, C4-THIQH), 3.50 (t, *J* = 5.9 Hz, 2H, C3-THIQH), 4.38 (s, 2H, C1-THIQH), 5.39 (s, 2H, CH<sub>2</sub>O), 6.30 (d, *J* = 9.5 Hz, 1H, ArH), 6.96–7.02 (m, 2H, ArH), 7.03–7.18 (m, 4H, ArH), 7.44 (d, *J* = 9.3 Hz, 1H, ArH), 7.68 (d, *J* = 9.5 Hz, 1H, ArH), 7.74 (t, *J* = 8.0 Hz, 1H, ArH), 7.93 (d, *J* = 8.0 Hz, 1H, ArH), 8.06 (d, *J* = 8.0 Hz, 1H, ArH), 8.17 (s, 1H, CHN), 8.20 (s, 1H, ArH). <sup>13</sup>C NMR (75 MHz, CDCl<sub>3</sub>) δ 28.6, 43.8, 47.5, 62.2, 102.2, 112.7, 113.2, 113.7, 119.3, 121.2, 124.5, 126.3, 126.5, 127.0, 127.6, 128.9, 129.0, 130.9, 131.1, 132.8, 137.4, 139.3, 143.2, 144.4, 155.8, 161.0, 161.1. HRMS-TOF: *m/z* [M+H]<sup>+</sup> 515.1390 (Calcd for C<sub>27</sub>H<sub>23</sub>N<sub>4</sub>O<sub>5</sub>S: 515.1384).

#### 4.6.2. 4-((1-(3-((3,4-Dihydroisoquinolin-2(1H)-yl)sulfonyl)phenyl)-1H-1,2,3-triazol-4-yl)methoxy)-2H-chromen-2-one (**33**)

White solid. 91%. Mp 168–170 °C. IR (UATR) cm<sup>-1</sup>: 1712, 1623, 1566, 1494, 1455, 1372, 1336, 1248, 1191, 1153. <sup>1</sup>H NMR (300 MHz, CDCl<sub>3</sub>) δ 2.95 (t, *J* = 5.9 Hz, 2H, C4-THIQH), 3.51 (t, *J* = 5.9 Hz, 2H, C3-THIQH), 4.40 (s, 2H, C1-THIQH), 5.47 (s, 2H, CH<sub>2</sub>O), 5.93 (s, 1H, CHCO), 7.04–7.20 (m, 4H, ArH), 7.30 (t, *J* = 7.6 Hz, 1H, ArH), 7.35 (d, *J* = 7.6 Hz, 1H, ArH), 7.59 (dd, *J* = 7.8, 1.6 Hz, 1H, ArH), 7.76 (t, *J* = 8.0 Hz, 1H, ArH), 7.85 (dt, *J* = 7.9, 1.5 Hz, 1H, ArH), 7.95 (d, *J* = 8.1 Hz, 2H, ArH), 8.08 (d, *J* = 8.1 Hz, 2H, ArH), 8.22, 8.23 (2s, 2H, ArH, CHN). <sup>13</sup>C NMR (75 MHz, CDCl<sub>3</sub>) δ 28.6, 43.8, 47.5, 62.5, 91.4, 115.4, 116.9, 119.4, 121.6, 123.1,

124.0, 124.6, 126.3, 126.6, 127.0, 127.8, 128.9, 131.0, 131.1, 132.7, 132.8, 137.3, 153.4, 162.5, 164.9. HRMS-TOF:  $m/z$  [M+H]<sup>+</sup> 515.1385 (Calcd for C<sub>27</sub>H<sub>23</sub>N<sub>4</sub>O<sub>5</sub>S: 515.1384).

#### 4.6.3. 7-((1-(3-((6,7-Dimethoxy-3,4-dihydroisoquinolin-2(1H)-yl)sulfonyl)phenyl)-1H-1,2,3-triazol-4-yl)methoxy)-2H-chromen-2-one (34)

White solid. 92%. Mp 180–181 °C. IR (UATR) cm<sup>-1</sup>: 1723, 1613, 1522, 1466, 1347, 1226, 1163, 1120. <sup>1</sup>H NMR (300 MHz, CDCl<sub>3</sub>) δ 2.86 (t,  $J$  = 5.8 Hz, 2H, C4-THIQH), 3.47 (t,  $J$  = 5.9 Hz, 2H, C3-THIQH), 3.83 (s, 6H, 2 × OCH<sub>3</sub>), 4.31 (s, 2H, C1-THIQH), 5.39 (s, 2H, CH<sub>2</sub>O), 6.30 (d,  $J$  = 9.5 Hz, 1H, ArH), 6.54, 6.56 (2s, 2H, ArH), 6.92–6.98 (m, 2H, ArH), 7.39 (d,  $J$  = 9.2 Hz, 1H, ArH), 7.63 (d,  $J$  = 9.5 Hz, 1H, ArH), 7.70 (t,  $J$  = 8.0 Hz, 1H, ArH), 7.87 (d,  $J$  = 7.8 Hz, 1H, ArH), 7.99 (d,  $J$  = 7.6 Hz, 1H, ArH), 8.13 (s, 1H, CHN), 8.17 (s, 1H, ArH). <sup>13</sup>C NMR (75 MHz, CDCl<sub>3</sub>) δ 28.2, 43.8, 47.2, 55.9, 56.0, 62.2, 102.2, 109.0, 111.5, 112.7, 113.2, 113.7, 119.4, 121.2, 122.9, 124.4, 124.8, 127.6, 129.0, 130.8, 137.3, 139.4, 143.2, 144.5, 147.9, 148.1, 155.8, 160.9, 161.1. HRMS-TOF:  $m/z$  [M+H]<sup>+</sup> 575.1589 (Calcd for C<sub>29</sub>H<sub>27</sub>N<sub>4</sub>O<sub>7</sub>S: 575.1595).

#### 4.6.4. 4-((1-(3-((6,7-Dimethoxy-3,4-dihydroisoquinolin-2(1H)-yl)sulfonyl)phenyl)-1H-1,2,3-triazol-4-yl)methoxy)-2H-chromen-2-one (35)

White solid. 90%. Mp 211–213 °C. IR (UATR) cm<sup>-1</sup>: 1717, 1622, 1518, 1457, 1384, 1343, 1238, 1156, 1114. <sup>1</sup>H NMR (300 MHz, CDCl<sub>3</sub>) δ 2.86 (t,  $J$  = 5.7 Hz, 2H, C4-THIQH), 3.48 (t,  $J$  = 5.7 Hz, 2H, C3-THIQH), 3.83 (s, 6H, 2 × OCH<sub>3</sub>), 4.35 (s, 2H, C1-THIQH), 5.48 (s, 2H, CH<sub>2</sub>O), 5.94 (s, 1H, CHCO), 6.54, 6.56 (2s, 2H, ArH), 7.29 (t,  $J$  = 7.7 Hz, 1H, ArH), 7.35 (d,  $J$  = 8.3 Hz, 1H, ArH), 7.59 (t,  $J$  = 7.6 Hz, 1H, ArH), 7.76 (t,  $J$  = 7.8 Hz, 1H, ArH), 7.85 (d,  $J$  = 7.9 Hz, 1H, ArH), 7.94 (d,  $J$  = 7.7 Hz, 1H, ArH), 8.07 (d,  $J$  = 7.6 Hz, 2H, ArH), 8.24 (s, 2H, ArH, CHN). <sup>13</sup>C NMR (75 MHz, CDCl<sub>3</sub>) δ 28.2, 43.9, 47.3, 55.9, 56.0, 62.5, 91.4, 108.9, 111.4, 115.4, 116.9, 119.5, 121.6, 122.9, 123.1, 124.0, 124.5, 124.8, 127.8, 130.9, 132.7, 137.2, 139.5, 142.9, 147.9, 148.1, 153.4, 162.5, 164.9. HRMS-TOF:  $m/z$  [M+H]<sup>+</sup> 575.1597 (Calcd for C<sub>29</sub>H<sub>27</sub>N<sub>4</sub>O<sub>7</sub>S: 575.1595).

#### 4.7. Aromatase inhibition assay

Aromatase inhibitory effect was performed using the modified method reported by Stessor et al.<sup>20</sup> This method was carried out according to the Gentest kit using CYP19 enzyme and *O*-benzyl fluorescein benzyl ester (DBF) as a fluorometric substrate. DBF was dealkylated by aromatase and then hydrolyzed to give the fluorescein product.

Briefly, 100 μL of cofactor, containing 78.4 μL of 50 mM phosphate buffer (pH 7.4); 20 μL of 20 × NADPH-generating system (26 mM NADP<sup>+</sup>, 66 mM glucose-6-phosphate, and 66 mM MgCl<sub>2</sub>); and 1.6 μL of 100 U/mL glucose-6-phosphate dehydrogenase, were pipetted into a 96-well black plate and preincubated in 37 °C (water bath) for 10 min. The reaction was initiated by addition of 100 μL of enzyme/substrate (E/S) mixture containing 77.3 μL of 50 mM phosphate buffer (pH 7.4); 12.5 μL of 16 pmol/mL CYP19; 0.2 μL of 0.2 mM DBF, and 10 μL of tested sample or 10% DMSO as a negative control or ketoconazole/letrozole as a positive control. Fluorescence signal was recorded using an excitation wavelength of 490 nm and emission wavelength of 530 nm with cutoff 515 nm. Percentage of inhibition (% inhibition) was calculated as shown in Eq. 1. Samples with % inhibition greater than 50 were further calculated according to Eq. 1 to obtain their IC<sub>50</sub> values.

$$\% \text{inhibition} = 100 - \left[ \frac{(\text{sample} - \text{blank})}{(\text{DMSO} - \text{blank})} \times 100 \right] \quad (1)$$

#### 4.8. Cytotoxicity assay: primate cell line (Vero)

The cytotoxicity was carried out by using the Green Fluorescent Protein (GFP) detection method.<sup>21</sup> The GFP-expressing Vero cell line was generated in-house by stably transfecting the African green monkey kidney cell line (Vero, ATCC CCL-81), with pEGFP-N1 plasmid (Clontech). The assay was performed by adding 45 μL of cell suspension at 3.3 × 10<sup>4</sup> cells/mL to each well of 384-well plates containing 5 μL of test compounds diluted in 0.5% DMSO. After incubation for 4 days in 37 °C incubator with 5% CO<sub>2</sub>. Fluorescence signals were measured using SpectraMax M5 microplate reader (Molecular Devices, USA) with excitation and emission wavelengths of 485 and 535 nm, respectively. IC<sub>50</sub> values were deduced from dose-response curves, using 6 concentrations of 3-fold serially diluted samples, by the SOFTMax Pro software (Molecular device). Ellipticine and 0.5% DMSO were used as a positive and a negative control, respectively.

#### 4.9. Molecular docking

Molecular docking was performed to elucidate interactions of investigated compounds toward its target protein namely the aromatase enzyme. Initially, the crystal structure of the human placental aromatase (cytochrome P450, member 19A1) co-crystallized with the androstenedione (ASD) substrate was retrieved from the Protein Data Bank (PDB ID: 3EQM). Investigated compounds (13–35) were constructed using Marvin Sketch version 6.0 and were geometrically optimized by Gaussian 09<sup>22</sup> using Becke's three-parameter hybrid method with the Lee–Yang–Parr correlation functional (B3LYP) together with the 6-31 g(d) basis set. Prior to docking, the protein structure was prepared by addition of H atoms and side chain repair using the WHAT IF software.<sup>23</sup> Subsequently, the Gasteiger and Kollman charges were added to the ligands (the co-crystallized ligand ASD and optimized compounds 13–35) and protein structures, respectively, using the PyRx 0.6 software.<sup>24</sup> A grid box with a size of 62.06 × 71.95 × 51.46 Å was created by the AutoGrid software to cover all area of aromatase. The center of the grid box was allocated using x, y, z coordinates of 83.4375, 50.1006 and 46.3803, respectively. Molecular docking was performed using AutoDock Vina, which is a part of the PyRx 0.6 software.<sup>24</sup> The co-crystallized ligand ASD was re-docked to aromatase as to validate the docking protocol. The re-docking was evaluated by the calculation of root mean standard deviation (RMSD) between the original and re-docked position of the co-crystallized ligand using the Chimera software.<sup>25</sup> Docking poses of investigated compounds (13–35) were visualized using the PyMoL software<sup>26</sup> and the ligand–protein interactions were generated using online available tool, PoseViewWeb version 1.97.0.<sup>27</sup>

#### Acknowledgments

This project is financially supported from Srinakharinwirot University and the Higher Education Research Promotion (HERP). R.P. is grateful for the Thailand Research Fund (MRG5680001). Great supports from the Office of Higher Education Commission and Mahidol University under the National Research Universities Initiative are appreciated. We are also indebted to Chulabhorn Research Institute for recording mass spectra and bioactivity testing.

#### Supplementary data

Supplementary data associated with this article can be found, in the online version, at <http://dx.doi.org/10.1016/j.bmc.2015.04.036>.

## References and notes

1. Palmieri, C.; Patten, D. K.; Januszewski, A.; Zucchini, G.; Howell, S. J. *Mol. Cell. Endocrinol.* **2014**, *382*, 695.
2. Gobbi, S.; Rampa, A.; Belluti, F.; Bisi, A. *Anticancer Agents Med. Chem.* **2014**, *14*, 54.
3. Favia, A. D.; Nicolotti, O.; Stefanachi, A.; Leonetti, F.; Carotti, A. *Expert Opin. Drug Discov.* **2013**, *8*, 395.
4. Agalave, S. G.; Maujan, S. R.; Pore, V. S. *Chem. Asian J.* **2011**, *6*, 2696.
5. Neves, M. A. C.; Dinis, T. C. P.; Colombo, G. J. *Med. Chem.* **2009**, *52*, 143.
6. Doiron, J.; Souttan, A. H.; Richard, R.; Touré, M. M.; Picot, N.; Richard, R.; Čuperlović-Culf, M.; Robichaud, G. A.; Touaibia, M. *Eur. J. Med. Chem.* **2011**, *46*, 4010.
7. Pingaew, R.; Prachayasittikul, S.; Ruchirawat, S.; Prachayasittikul, V. *Med. Chem. Res.* **2014**, *23*, 1768.
8. Pingaew, R.; Mandi, P.; Nantasenamat, C.; Prachayasittikul, S.; Ruchirawat, S.; Prachayasittikul, V. *Eur. J. Med. Chem.* **2014**, *81*, 192.
9. Ghosh, D.; Griswold, J.; Erman, M.; Pangborn, W. *Nature* **2009**, *457*, 219.
10. Recanatini, M.; Bisi, A.; Cavalli, A.; Belluti, F.; Gobbi, S.; Rampa, A.; Valenti, P.; Palzer, M.; Paluszczak, A.; Hartmann, R. W. *J. Med. Chem.* **2001**, *44*, 672.
11. Stefanachi, A.; Favia, A. D.; Nicolotti, O.; Leonetti, F.; Pisani, L.; Catto, M.; Zimmer, C.; Hartmann, R. W.; Carotti, A. *J. Med. Chem.* **2011**, *54*, 1613.
12. Kao, Y.-C.; Korzekwa, K. R.; Loughton, C. A.; Chen, S. *Eur. J. Biochem.* **2001**, *268*, 243.
13. Abadi, A. H.; Abou-Seri, S. M.; Hu, Q.; Negri, M.; Hartmann, R. W. *MedChemComm* **2012**, *3*, 663.
14. Cavalli, A.; Recanatini, M. *J. Med. Chem.* **2002**, *45*, 251.
15. Wood, P. M.; Woo, L. W. L.; Thomas, M. P.; Mahon, M. F.; Purohit, A.; Potter, B. V. L. *ChemMedChem* **2011**, *6*, 1423.
16. Narayana, B. L.; Kishore, D. P.; Balakumar, C.; Rao, K. V.; Kaur, R.; Rao, A. R.; Murthy, J. N.; Ravikumar, M. *Chem. Biol. Drug Des.* **2012**, *79*, 674.
17. Bonfield, K.; Amato, E.; Bankemper, Y.; Agard, H.; Steller, J.; Keeler, J. M.; Roy, D.; McCallum, A.; Paula, S.; Ma, L. *Bioorg. Med. Chem.* **2012**, *20*, 2603.
18. Pingaew, R.; Prachayasittikul, S.; Ruchirawat, S.; Prachayasittikul, V. *Med. Chem. Res.* **2013**, *22*, 267.
19. Jamieson, S. M. F.; Brooke, D. G.; Heinrich, D.; Atwell, G. J.; Silva, S.; Hamilton, E. J.; Turnbull, A. P.; Rigoreau, L. J. M.; Trivier, E.; Soudy, C.; Samlal, S. S.; Owen, P. J.; Schroeder, E.; Raynham, T.; Flanagan, J. U.; Denny, W. A. *J. Med. Chem.* **2012**, *55*, 7746.
20. Stresser, D. M.; Turner, S. D.; McNamara, J.; Stocker, P.; Miller, V. P.; Crespi, C. L.; Patten, C. J. *Anal. Biochem.* **2000**, *284*, 427.
21. Hunt, L.; Jordan, M.; De Jesus, M.; Wurm, F. M. *Biotechnol. Bioeng.* **1999**, *65*, 201.
22. Frisch, M. J.; Trucks, G. W.; Schlegel, H. B.; Scuseria, G. E.; Robb, M. A.; Cheeseman, J. R.; Scalmani, G.; Barone, V.; Mennucci, B.; Petersson, G. A.; Nakatsuji, H.; Caricato, M.; Li, X.; Hratchian, H. P.; Izmaylov, A. F.; Bloino, J.; Zheng, G.; Sonnenberg, J. L.; Hada, M.; Ehara, M.; Toyota, K.; Fukuda, R.; Hasegawa, J.; Ishida, M.; Nakajima, T.; Honda, Y.; Kitao, O.; Nakai, H.; Vreven, T.; Peralta, J. A. M. Jr., J. E.; Ogliaro, F.; Bearpark, M.; Heyd, J. J.; Brothers, E.; Kudin, K. N.; Staroverov, V. N.; Kobayashi, R.; Normand, J.; Raghavachari, K.; Rendell, A.; Burant, J. C.; Iyengar, S. S.; Tomasi, J.; Cossi, M.; Rega, N.; Millam, J. M.; Klene, M.; Knox, J. E.; Cross, J. B.; Bakken, V.; Adamo, C.; Jaramillo, J.; Gomperts, R.; Stratmann, R. E.; Yazyev, O.; Austin, A. J.; Cammi, R.; Pomelli, C.; Ochterski, J. W.; Martin, R. L.; Morokuma, K.; Zakrzewski, V. G.; Voth, G. A.; Salvador, P.; Dannenberg, J. J.; Dapprich, S.; Daniels, A. D.; Farkas, Ö.; Foresman, J. B.; Ortiz, J. V.; Cioslowski, J.; Fox, D. J. Gaussian, Inc., Wallingford CT, 2009.
23. Vriend, G. *J. Mol. Graphics* **1990**, *8*, 52.
24. Dallakyan, S. PyRx Version 0.6., 2013. <http://pyrx.scripps.edu>.
25. Pettersen, E. F.; Goddard, T. D.; Huang, C. C.; Couch, G. S.; Greenblatt, D. M.; Meng, E. C.; Ferrin, T. E. *J. Comput. Chem.* **2004**, *25*, 1605.
26. Delano, W. *PyMOL Release 0.99*; DeLano Scientific LLC: Palo Alto, CA, 2002.
27. Stierand, K.; Rarey, M. *ACS Med. Chem. Lett.* **2010**, *1*, 540.